

A Joint Communication and Control System for URLLC in Industrial IoT

Yizhe Zhao, *Member, IEEE*, Jie Hu, *Senior Member, IEEE*, Kun Yang, *Fellow, IEEE* and Xiaohui Wei

Abstract—Ultra reliable low latency communication (URLLC) is playing an important role in future wireless networks, such as industrial Internet of things (IIoT). Enormous industrial devices are requiring instant and highly-frequent control services, namely delay sensitive control, in order to improve the human safety or the operation accuracy. In this paper, a joint communication and delay sensitive control (JCDSC) system with URLLC is studied, where the control intervals are much shorter than the transmission latency. The control performance, known as the mean square error (MSE) of the plant states, are analysed in theory. The optimal blocklength of the control codewords, the data rate, as well as the minimum required control periods are then obtained, in order to minimize the control latency. Simulation results validate our theoretical analysis, while also demonstrating that an optimal blocklength of codewords should be selected in order to reduce the control latency.

Index Terms—URLLC, joint communication and control, IIoT, performance analysis

I. INTRODUCTION

Ultra reliable low latency communication (URLLC) [1] [2] has been considered as a promising technology in the future 6G, where various devices are much sensitive to the transmission delay of high quality services. The reduction of the latency is booming more potential technologies, such as digital twin aided mobile edge computing [3]. Meanwhile, the improvement of the reliability is also essential in the heterogeneous ultra-dense networks [4]. Some URLLC aided typical scenarios have been studied, such as the metaverse [5], vehicular networks [6], industrial Internet of things (IIoT) [7], in which the inner plants all require instant control services. For instance, motors require accurate motion controls to guarantee the human safety, while unmanned ariel vehicles (UAVs) and the intelligent mechanical arms in the IIoT also requires accurate controls. Central units, such as base stations (BSs) and access points (APs), are relied upon for providing remote control services to the plants via wireless channels, which is known as joint communication and control [8].

Yizhe Zhao, Jie Hu are with the School of Information and Communication Engineering, University of Electronic Science and Technology of China, Chengdu, China, email: yzzhao@uestc.edu.cn, hujie@uestc.edu.cn.

Kun Yang is with the School of Information and Communication Engineering, University of Electronic Science and Technology of China, Chengdu 611731, China, and also with the School of Computer Science and Electronic Engineering, University of Essex, Colchester, CO4 3SQ, U.K., email: kyang@ieee.org.

Xiaohui Wei is with the School of Computer Science and Technology, Jilin University, Changchun, China, email: weixh@jlu.edu.cn.

This work is supported in part by the Natural Science Foundation of China (Grant No. 62132004, Grant No. 61971102, No. 62201123, No. U19A2061 and No. 62272190), MOST Major Research and Development Project (Grant No.: 2021YFB2900204), Sichuan Major R&D Project (Grant No.: 22QYCX0168) and Sichuan Science and Technology Program (Grant No. 2022YFH0022), and in part by the Municipal Government of Quzhou (Grant No.: 2022D031), EU H2020 Project COSAFE (GA-824019) and China Postdoctoral Science Foundation (Grant No. 2022TQ0056).

Recently, lots of works [9]–[14] have focused on the joint communication and control design. For instance, Hong *et.al* [9] studied a design of platoon communication and control in a vehicular to vehicular (V2V) system, in order to reduce the position errors of vehicles. Chang *et.al* [10] studied a URLLC assisted real-time wireless control system, where an autonomous device-to-device (D2D) communication scheme was developed. Then, in his later work [11], the UAV motion control in a Tera-Hertz (THz) cellular system was studied, where joint sensing, communication and control design was obtained for improving the communication quality of the back-haul links from the UAV to the BS. In the IIoT scenario, Liu *et.al* [12] analysed the performance of a wireless networked control system, while the optimal system design was also studied for minimizing the infinite control mean square error (MSE) between the real plant state and the default plant state. Furthermore, the age of information (AoI) for the joint communication and control in the IIoT was analysed in [13], while an optimal control strategy was also proposed.

Although these works studied the impact of transmission latency on the control performance, they did not consider the delay sensitive control. In the industrial scenario, due to the low-latency requirements, some plants are updated more frequently and the interval between two control operations may be much shorter than the transmission latency. Therefore, during the transmission of the controlling signals, the plant states are updated many times and are influenced by the additive control noise, which may seriously degrade the control performance. Consequently, the control signal should be generated by estimating the updated plant state before the next control operation occurs. In order to address this problem, joint communication and delay sensitive control (JCDSC) should be investigated for unveiling their coupling relationship. Liu *et.al* [15] studied the tradeoff among the latency, reliability and rate in wireless delay sensitive controlled networks. Nevertheless, the detailed control performance during JCDSC was not analysed. Against this background, our contributions are summarised as follows:

- We study a JCDSC system in the industrial scenario, where the control interval is much shorter than the transmission latency. The control performance is influenced by the additive control noise during the transmission of the control signal, which is generated by estimating the updated plant state before the next control operation occurs. The MSE of the plant states are analysed in theory as a control performance metric.
- We optimize the blocklength of the control codeword as well as the data rate for minimizing the control latency, by ensuring that the average control MSE of the plant is

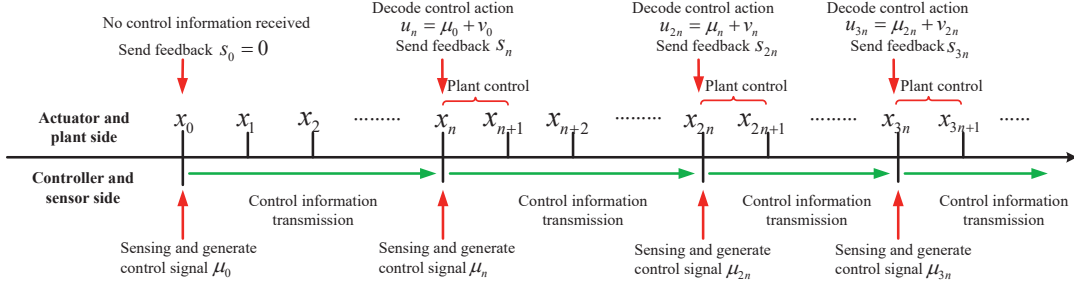


Fig. 2. Timeline illustration of the joint communication and control system.

further quantized and encoded into a specific codeword. By denoting the overall quantization range of the control signal as $[-H, H]$, the quantization interval for each codeword is derived as $\Delta = H/2^{nR-1}$, where each codeword corresponds to a specific quantized range of the control signal. Then, the encoded control codeword is transmitted to the actuator in the next n time-slots, while the recovered control action u_{t+n} at time-slot $(t+n)$ is expressed as

$$u_{t+n} = \begin{cases} \mu_t + v_t, & t = kn, k \in \mathbb{Z}_0, s_{t+n} = 1, \\ 0, & \text{otherwise,} \end{cases} \quad (6)$$

where \mathbb{Z}_0 represents a nonnegative integer set, v_t represents the quantization noise caused by the (nR) -bit quantizer at time-slot t . It's assumed that v_t follows a uniform distribution within a range of $[-\Delta/2, \Delta/2]$.

Due to the control latency of n time-slots, the control signal μ_t at time-slot $t = kn$ should be generated by estimating the plant state \bar{x}_{t+n} at time-slot $(t+n)$. By adopting the classic linear-quadratic-Gaussian (LQG) control method in [15], the control signal μ_t is generated as

$$\mu_t = -a\bar{x}_{t+n}/b, \quad (7)$$

where the estimated plant state \bar{x}_{t+n} is formulated as

$$\bar{x}_{t+n} = \begin{cases} a^n x_t, & t = kn, k \in \mathbb{Z}_0, s_t = 0, \\ a^{n-1}(ax_t + b\mu_{t-n}), & t = kn, k \in \mathbb{Z}_0, s_t = 1. \end{cases} \quad (8)$$

III. PERFORMANCE ANALYSIS OF THE JCDSK SYSTEM

The control MSE of the plant at time-slot t ($t \in \mathbb{Z}_0$) is defined as $J_t = \mathbb{E}[|x_t|^2] = \mathbb{E}[|\hat{x}_t - \bar{x}|^2]$, which is the mean square error of the difference between the default state \bar{x} and the current state \hat{x}_t of the plant at time-slot t . If $J_t = 0$, the plant is perfectly controlled. In order to reduce the influence of the redundant signals caused by the blocklength information interaction, we assume that the blocklength of the control codeword keeps as a constant n until the control goal is achieved. In this section, the control MSE J_t of all the plants will be analysed for the further optimization. By separating the timeline into periods, where the $(k+1)$ -th periods refers to the time-slot range of $[kn+1, (k+1)n]$, J_t is further analysed as follows. It is also assumed that the SNR remains as a constant in different periods, since the controller is able to operate dynamic power allocation for the control signals' transmission to keep the SNR unchanged.

A. Case I: $t \neq kn+1$ ($k \in \mathbb{Z}_0$)

Since we have $u_t = 0$ for any $t \neq kn$, the plant state of x_t in Case I can be simplified as

$$x_t = ax_{t-1} + w_{t-1}. \quad (9)$$

By denoting $t = kn+i$ where $i = 2, \dots, n$, the plant state x_{kn+i} can be reformulated as

$$\begin{aligned} x_{kn+i} &= ax_{kn+i-1} + w_{kn+i-1} \\ &= \dots = a^{i-1}x_{kn+1} + \sum_{j=0}^{i-2} a^j w_{kn+i-1-j}. \end{aligned} \quad (10)$$

Since the control noise w_t is independent among time-slots, the control MSE at time-slot $(kn+i)$ is derived as

$$\begin{aligned} J_{kn+i} &= \mathbb{E} \left[\left| a^{i-1}x_{kn+1} + \sum_{j=0}^{i-2} a^j w_{kn+i-1-j} \right|^2 \right] \\ &= a^{2(i-1)}J_{kn+1} + \frac{1-a^{2(i-1)}}{1-a^2}\sigma_w^2. \end{aligned} \quad (11)$$

B. Case II: $t = kn+1$ ($k \in \mathbb{Z}_0$)

In order to analyse the control MSE at time-slot $t = kn+1$ ($k \in \mathbb{Z}_0$), three sub-cases are further studied by considering $k = 0, k = 1$ and $k \geq 2$, respectively.

1) *Case II-1: $k = 0$* : Since no control information is received at time-slot $t = 1$, the plant state x_1 is expressed as $x_1 = ax_0 + w_0$, where x_0 is the initial plant state. Therefore, the control MSE at time-slot $t = 1$ is formulated as

$$J_1 = a^2J_0 + \sigma_w^2. \quad (12)$$

2) *Case II-2: $k = 1$* : According to Eqs. (1), (6), (7) and (9), the plant state x_{kn+1} at time-slot $t = kn+1$ ($k > 0$) can be reformulated as

$$\begin{aligned} x_{kn+1} &= ax_{kn} + bu_{kn} + w_{kn} \\ &= \begin{cases} ax_{kn} + b\mu_{(k-1)n} + bv_{(k-1)n} + w_{kn}, & s_{kn} = 1, \\ ax_{kn} + w_{kn}, & s_{kn} = 0. \end{cases} \\ &= \begin{cases} ax_{kn} - a\bar{x}_{kn} + bv_{(k-1)n} + w_{kn}, & s_{kn} = 1, \\ a^n x_{(k-1)n+1} + \sum_{j=0}^{n-1} a^j w_{kn-j}, & s_{kn} = 0. \end{cases} \end{aligned} \quad (13)$$

According to Eq. (8), the estimated plant state \bar{x}_{kn} is also related to the decoding result of $u_{(k-1)n}$. Therefore, Eq. (13) can be further formulated as

$$x_{kn+1} = \begin{cases} \sum_{j=0}^n a^j w_{kn-j} + bv_{(k-1)n}, & s_{kn} = 1, s_{(k-1)n} = 0, \\ \sum_{j=0}^n a^j w_{kn-j} + bv_{(k-1)n} + a^n bv_{(k-2)n}, & s_{kn} = 1, s_{(k-1)n} = 1, \\ a^n x_{(k-1)n+1} + \sum_{j=0}^{n-1} a^j w_{kn-j}, & s_{kn} = 0. \end{cases} \quad (14)$$

Since no control signal is received at time-slot $t = 0$, we have $s_0 = 0$. Therefore, the plant state x_{n+1} is expressed as

$$x_{n+1} = \begin{cases} \sum_{j=0}^n a^j w_{n-j} + bv_0, & s_n = 1, \\ a^n x_1 + \sum_{j=0}^{n-1} a^j w_{n-j}, & s_n = 0. \end{cases} \quad (15)$$

Assuming a uniformly distributed random variable v_t within the range of $[-\Delta/2, \Delta/2]$, the variance of $\mathbb{E}[|v_t|^2]$ is derived as

$$\mathbb{E}[|v_t|^2] = \int_{-\Delta/2}^{\Delta/2} \frac{1}{\Delta} v_t^2 dv_t = \frac{H^2}{3 \cdot 2^{2nR}}. \quad (16)$$

Considering the BLER ϵ of the control action u_n , the control MSE J_{n+1} is formulated as

$$\begin{aligned} J_{n+1} &= (1 - \epsilon) \left(\frac{1 - a^{2(n+1)}}{1 - a^2} \sigma_w^2 + \frac{b^2 H^2}{3 \cdot 2^{2nR}} \right) \\ &\quad + \epsilon \left(a^{2n} J_1 + \frac{1 - a^{2n}}{1 - a^2} \sigma_w^2 \right) \\ &= \epsilon a^{2(n+1)} J_0 + \frac{(1 - \epsilon) b^2 H^2}{3 \cdot 2^{2nR}} + \frac{1 - a^{2(n+1)}}{1 - a^2} \sigma_w^2. \end{aligned} \quad (17)$$

3) *Case II-3: $k \geq 2$* : According to Eq. (14), the plant state x_{kn+1} is not only related to the decoding result of u_{kn} , but also related to that of $u_{(k-1)n}$. Denoting l as the number of the consecutive periods in which the control actions are all decoded incorrectly, which ends in the $(k+1)$ -th period, three more cases are further considered as follows.

- *Case II-3-1: $l = k$* . In this case, all the control actions from time-slot $t = 0$ suffer from the decoding failure. Its occurrence probability is expressed as $p_k = \epsilon^k$, while the plant state x_{kn+1} is reformulated as

$$x_{kn+1} = a^{(kn+1)} x_0 + \sum_{j=0}^{kn} a^j w_{kn-j}. \quad (18)$$

Therefore, the control MSE $J_{kn+1}^{(k)}$ in the case of $l = k$ is derived as

$$J_{kn+1}^{(k)} = a^{2(kn+1)} J_0 + \frac{1 - a^{2(kn+1)}}{1 - a^2} \sigma_w^2. \quad (19)$$

- *Case II-3-2: $l = k - 1$* . In this case, the control action u_n is decoded successfully, while all the following control actions u_{jn} ($j = 2, \dots, k$) suffer from the decoding failure. The probability of this case is expressed as

$p_{k-1} = (1 - \epsilon)\epsilon^{k-1}$, while the plant state x_{kn+1} is reformulated as

$$\begin{aligned} x_{kn+1} &= a^{(k-1)n} x_{n+1} + \sum_{j=0}^{(k-1)n-1} a^j w_{kn-j} \\ &= a^{(k-1)n} bv_0 + \sum_{j=0}^{kn} a^j w_{kn-j}. \end{aligned} \quad (20)$$

Then, the control MSE $J_{kn+1}^{(k-1)}$ in the case of $l = k - 1$ is derived as

$$\begin{aligned} J_{kn+1}^{(k-1)} &= a^{2(k-1)n} \left(\frac{1 - a^{2(n+1)}}{1 - a^2} \sigma_w^2 + \frac{b^2 H^2}{3 \cdot 2^{2nR}} \right) \\ &\quad + \frac{1 - a^{2(k-1)n}}{1 - a^2} \sigma_w^2 \\ &= \frac{1 - a^{2(kn+1)}}{1 - a^2} \sigma_w^2 + \frac{a^{2(k-1)n} b^2 H^2}{3 \cdot 2^{2nR}}. \end{aligned} \quad (21)$$

- *Case II-3-3: $0 \leq l < k - 1$* . In this case, the control action $u_{(k-l)n}$ is decoded successfully, while all the following control actions u_{jn} ($j = k - l + 1, \dots, k$) suffer from the decoding failure. The probability of this case is expressed as $p_l = (1 - \epsilon)\epsilon^l$, while the plant state x_{kn+1} is reformulated as

$$\begin{aligned} x_{kn+1} &= a^{ln} x_{(k-l)n+1} + \sum_{j=0}^{ln-1} a^j w_{kn-j} \\ &= \begin{cases} a^{ln} \left(\sum_{j=0}^n a^j w_{(k-l)n-j} + bv_{(k-l-1)n} \right) \\ \quad + \sum_{j=0}^{ln-1} a^j w_{kn-j}, & s_{(k-l-1)n} = 0, \\ a^{ln} \left(\sum_{j=0}^n a^j w_{(k-l)n-j} + bv_{(k-l-1)n} \right) \\ \quad + a^n bv_{(k-l-2)n} + \sum_{j=0}^{ln-1} a^j w_{kn-j}, & s_{(k-l-1)n} = 1. \end{cases} \end{aligned} \quad (22)$$

Since the control action $u_{(k-l-1)n}$ is independently decoded, the control MSE J_{kn+1}^l in Case II-3-3 is derived as

$$\begin{aligned} J_{kn+1}^{(l)} &= \frac{1 - a^{2((l+1)n+1)}}{1 - a^2} \sigma_w^2 + \frac{a^{2ln} b^2 H^2}{3 \cdot 2^{2nR}} \\ &\quad + (1 - \epsilon) \frac{a^{2(l+1)n} b^2 H^2}{3 \cdot 2^{2nR}} \end{aligned} \quad (23)$$

In summary, the control MSE J_{kn+1} at time-slot $t = kn + 1$ ($k \geq 2$) is derived as $J_{kn+1} = \sum_{l=0}^k p_l J_{kn+1}^{(l)}$.

C. Average Control MSE

In the first K periods, the overall control MSE $J_{tot,K}$ from time-slot $t = 1$ to time-slot $t = Kn$ is formulated as

$$\begin{aligned} J_{tot,K} &= \sum_{k=0}^{K-1} \sum_{i=1}^n J_{kn+i} \\ &= \sum_{k=0}^{K-1} \frac{1 - a^{2n}}{1 - a^2} J_{kn+1} + \frac{K \sigma_w^2}{1 - a^2} \left(n - \frac{1 - a^{2n}}{1 - a^2} \right), \end{aligned} \quad (24)$$

while the average control MSE $J_{avr,K}$ is expressed as $J_{avr,K} = J_{tot,K}/Kn$.

IV. DELAY SENSITIVE DESIGN

We study the JCDSC system with a higher initial MSE $\mathbb{E}[|x_0|^2]$. Denoting $D = nR$ as the required information bits for quantizing the control signal μ_t , we aim to obtain the optimal codeword blocklength n and the data rate R (or D), in order to minimize the control latency Kn for achieving the average control MSE threshold $J_{avr,th}$ and for realizing the delay sensitivity. Then, the optimization problem is formulated as

$$(P1) \min_{K,n,D} Kn \quad (25)$$

$$\text{s.t. } J_{avr,K} \leq J_{avr,th}, \quad (25a)$$

$$J_{avr,k} \geq J_{avr,k+1}, \quad k = 1, \dots, K_{th} \quad (25b)$$

$$\epsilon a^{2n} + (1 - \epsilon) \frac{a^{2n}}{2^{2D}} < 1, \quad (25c)$$

$$K, n, D \in \mathbb{Z}_+, \quad (25d)$$

$$D < nC, \quad (25e)$$

$$Kn \leq N_{max}, \quad (25f)$$

where \mathbb{Z}_+ denote the set of positive integers, N_{max} is the maximum tolerant time slot number for constraining the control MSE lower than the threshold, which is dependent on the urgency of the industrial tasks. Constraint (25b) ensures that the control MSE should monotonically decrease, in order to achieve the efficient control, where $K_{th} > K$ is a tolerant period number. Constraint (25c) stabilizes the plant in the mean-square sense, *i.e.* $\lim_{t \rightarrow \infty} \mathbb{E}[|x_t|^2] < \infty$, which is described in [15].

Note that (P1) is an integer programming problem and we are able to obtain the optimal solution with the aid of the exhaustive searching method. Observe from (25f) that the upper bound of n and K is $n_{UP} = K_{UP} = N_{max}$. According to (25e), the upper searching bound of D is derived as $D_{UP} = \lfloor n_{up}C \rfloor$. Moreover, according to the MSE analysis in Section III, the average MSE $J_{avr,K}$ decreases with K . Therefore, given n, D , the optimal K can be obtained within the range of $[1, K_{UP}]$ based on the bisection method, which has the complexity of $\mathcal{O}(\log_2 K_{UP})$. Then, the overall complexity of the searching method is around $\mathcal{O}(D_{UP}n_{UP} \log_2 K_{UP}) = \mathcal{O}(Cn_{UP}^2 \log_2 K_{UP})$.

V. NUMERICAL RESULTS

In this section, Monte Carlo based simulation is exploited for validating and evaluating the control performance of our JCDSC system. The duration of each time slot is $T = 1ms$. The plant constants are set to $a = 1.1$ and $b = 1$, while the variance of the Gaussian distributed control noise is $\sigma_w^2 = 0.001$. The initial plant state is set to $x_0 = 2.7$ and the quantization range of the control signal is $[-1000, 1000]$. The upper bound of n and K is set to $N_{max} = 300$. Without additional statement, the estimated SNR of the control signal's transmission is $\bar{\gamma} = 10$ dB, the SNR error is set to $\Delta\gamma = -20$ dB, and the codeword blocklength is $n = 10$.

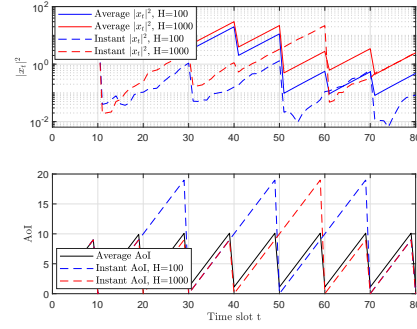


Fig. 3. Control process of the plant state and the control AoI.

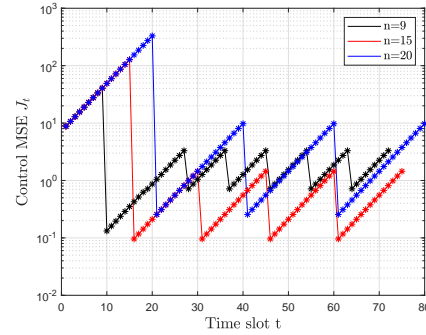


Fig. 4. Control MSE J_t versus time-slots. The markers represent the simulation results, while the curves represent the theoretical results.

In Fig. 3, we plot both the instant values and the average values of the control square error $|x_t|^2$ as well as the AoI with simulation. Note that the average value of the control square error is the so-called control MSE. The quantization range is set as $H = 100$ and $H = 1000$ respectively, while a larger H indicates a more serious quantization error. In the simulation, we set the BLER as $\epsilon = 0.2$ to observe instant values of control square error and the AoI (caused by the success or failure of the decoding of the control signals). Note that in practice, the BLER should be a much smaller value, in order to achieve efficient control. The instant values of AoI are plotted separately in two curves with different H , corresponding to the curves of the instant control square error $|x_t|^2$. Observe from Fig. 3 that the average AoI fluctuates periodically for every n time slots, while the control MSE appears a dentate decreasing trend. If the decoding error of the control signal occurs (such as the case of $H = 1000$ between the 40-th and the 60-th time slots), the instant AoI as well as the instant control square error increases continuously. Moreover, a larger H results in a higher control MSE, which indicates that a more serious quantization error results in a worse control performance.

We validate the analysis of the control performance of the JCDSC system in Fig. 4, where the data rate is set to $R = 1.2$ bits/channel use. Observe from Fig. 4 that the theoretical results perfectly match the simulation results. With time goes on, the control MSE J_t firstly decreases by periods and then achieves a convergence. Within a period which is defined in Section III, J_t exhibits an exponentially increasing trend, since no control action is received at the plant. Moreover, the control MSE when the codeword blocklength is $n = 15$ outperforms

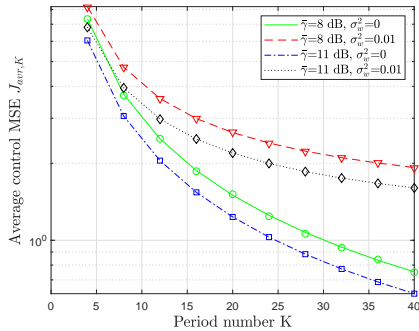


Fig. 5. Average control MSE $J_{avr,K}$ versus period number K . The markers represent the simulation results, while the curves represent the theoretical results.

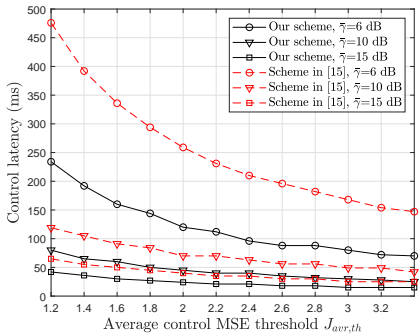


Fig. 6. Control latency versus average control MSE threshold $J_{avr,th}$, when compared to the scheme in [15].

the other benchmarks. This is because a longer codeword blocklength n results in a higher average J_t within a period. However, if n is very small, the system suffers much from a higher BLER ϵ , which results in more control failures and a higher control MSE.

Fig. 5 depicts the average control MSE $J_{avr,K}$ versus the period number K . Observe from Fig. 5 that when the number of periods increases, the average control MSE in K periods decreases. A higher control noise variance results in a higher $J_{avr,K}$. Moreover, when the SNR of the control signal's transmission increases, $J_{avr,K}$ reduces. This is because a higher SNR may reduce the BLER ϵ , which further results in a better control performance.

Fig. 6 depicts the comparison of the control latency performance between our optimization scheme and the scheme in [15]. Observe from Fig. 6 that our scheme outperforms the benchmark on the latency performance, since we aim to minimize the overall latency for the delay sensitive control. When we increase the SNR of the control signal's transmission, the control latency decreases, since a higher SNR $\tilde{\gamma}$ results in a lower BLER ϵ . Therefore, we are able to select a smaller n to reduce the control MSE. Moreover, when the average control MSE threshold $J_{avr,th}$ becomes higher, the control latency reduces, since it requires less time to achieve the control goal.

VI. CONCLUSION

A joint communication and delay sensitive control system is studied in this paper, where the control interval is much shorter than the transmission latency. The average control MSE is then

analysed in the closed-form. In order to reduce the control latency, the optimal codeword blocklength, the data rate and the number of periods are all obtained. Simulation results validate our theoretical analysis, which also demonstrate that an optimal blocklength of codewords should be selected in order to reduce the control latency.

REFERENCES

- [1] G. J. Sutton, J. Zeng, R. P. Liu, W. Ni, D. N. Nguyen, B. A. Jayawickrama, X. Huang, M. Abolhasan, Z. Zhang, E. Dutkiewicz, and T. Lv, "Enabling technologies for ultra-reliable and low latency communications: From phy and mac layer perspectives," *IEEE Communications Surveys and Tutorials*, vol. 21, no. 3, pp. 2488–2524, 2019.
- [2] C. She, C. Sun, Z. Gu, Y. Li, C. Yang, H. V. Poor, and B. Vucetic, "A tutorial on ultrareliable and low-latency communications in 6g: Integrating domain knowledge into deep learning," *Proceedings of the IEEE*, vol. 109, no. 3, pp. 204–246, 2021.
- [3] W. Sun, H. Zhang, R. Wang, and Y. Zhang, "Reducing offloading latency for digital twin edge networks in 6G," *IEEE Transactions on Vehicular Technology*, vol. 69, no. 10, pp. 12 240–12 251, 2020.
- [4] W. Sun, L. Wang, J. Liu, N. Kato, and Y. Zhang, "Movement aware CoMP handover in heterogeneous ultra-dense networks," *IEEE Transactions on Communications*, vol. 69, no. 1, pp. 340–352, 2021.
- [5] Z. Meng, C. She, G. Zhao, and D. D. Martini, "Sampling, communication, and prediction co-design for synchronizing the real-world device and digital model in metaverse," *CoRR*, vol. abs/2208.04233, 2022. [Online]. Available: <https://doi.org/10.48550/arXiv.2208.04233>
- [6] H. Khelifi, S. Luo, B. Nour, H. Mounqila, Y. Faheem, R. Hussain, and A. Ksentini, "Named data networking in vehicular ad hoc networks: State-of-the-art and challenges," *IEEE Communications Surveys and Tutorials*, vol. 22, no. 1, pp. 320–351, 2020.
- [7] Y. Wu, H.-N. Dai, H. Wang, Z. Xiong, and S. Guo, "A survey of intelligent network slicing management for industrial iot: Integrated approaches for smart transportation, smart energy, and smart factory," *IEEE Communications Surveys and Tutorials*, vol. 24, no. 2, pp. 1175–1211, 2022.
- [8] P. Park, S. Coleri Ergen, C. Fischione, C. Lu, and K. H. Johansson, "Wireless network design for control systems: A survey," *IEEE Communications Surveys and Tutorials*, vol. 20, no. 2, pp. 978–1013, 2018.
- [9] C. Hong, H. Shan, M. Song, W. Zhuang, Z. Xiang, Y. Wu, and X. Yu, "A joint design of platoon communication and control based on lte-v2v," *IEEE Transactions on Vehicular Technology*, vol. 69, no. 12, pp. 15 893–15 907, 2020.
- [10] B. Chang, L. Li, G. Zhao, Z. Chen, and M. A. Imran, "Autonomous D2D transmission scheme in URLLC for real-time wireless control systems," *IEEE Transactions on Communications*, vol. 69, no. 8, pp. 5546–5558, 2021.
- [11] B. Chang, W. Tang, X. Yan, X. Tong, and Z. Chen, "Integrated scheduling of sensing, communication, and control for mmwave/thz communications in cellular connected uav networks," *IEEE Journal on Selected Areas in Communications*, vol. 40, no. 7, pp. 2103–2113, 2022.
- [12] W. Liu, P. Popovski, Y. Li, and B. Vucetic, "Wireless networked control systems with coding-free data transmission for industrial IoT," *IEEE Internet of Things Journal*, vol. 7, no. 3, pp. 1788–1801, 2020.
- [13] X. Wang, C. Chen, J. He, S. Zhu, and X. Guan, "Aoi-aware control and communication co-design for industrial iot systems," *IEEE Internet of Things Journal*, vol. 8, no. 10, pp. 8464–8473, 2021.
- [14] M. Kligel, M. Mamduhi, O. Ayan, M. Vilgelm, K. H. Johansson, S. Hirche, and W. Kellerer, "Joint cross-layer optimization in real-time networked control systems," *IEEE Transactions on Control of Network Systems*, vol. 7, no. 4, pp. 1903–1915, 2020.
- [15] W. Liu, G. Nair, Y. Li, D. Nesić, B. Vucetic, and H. V. Poor, "On the latency, rate, and reliability tradeoff in wireless networked control systems for IIoT," *IEEE Internet of Things Journal*, vol. 8, no. 2, pp. 723–733, 2021.
- [16] Y. Polyanskiy, H. V. Poor, and S. Verdú, "Channel coding rate in the finite blocklength regime," *IEEE Transactions on Information Theory*, vol. 56, no. 5, pp. 2307–2359, 2010.
- [17] S. Schiessl, J. Gross, M. Skoglund, and G. Caire, "Delay performance of the multiuser MISO downlink under imperfect CSI and finite-length coding," *IEEE Journal on Selected Areas in Communications*, vol. 37, no. 4, pp. 765–779, 2019.